

EXPERIMENTAL INVESTIGATION OF ASYMPTOTIC MODAL ANALYSIS FOR A RECTANGULAR PLATE

Y. KUBOTA† AND E. H. DOWELL

School of Engineering, Duke University, Durham, North Carolina 27706, U.S.A.

(Received 2 February 1985, and in revised form 11 May 1985)

Experimental investigations of the response of a rectangular plate under a point random force have been performed to verify the asymptotic behavior predicted by Asymptotic Modal Analysis (AMA). Measurements have been made for various frequency bandwidths, center frequencies, and locations of the point force. The experimental results approach the results predicted by AMA as the frequency bandwidth becomes large. Moreover, experimental results show that the responses at all points of the plate except for some special areas become the same as the frequency bandwidth becomes large. However, the ratio of experimental results to AMA results has a greater variation from unity when the location of the point force is near the edge of the plate, than when the location of the point force is at the center of the plate. All experimental results show good agreement with the expected results from AMA.

1. INTRODUCTION

Dowell [1] showed that the results commonly referred to as Statistical Energy Analysis (SEA) [2] can be obtained by studying the asymptotic behavior of Classical Modal Analysis (CMA) for a general, linear structural system; those asymptotic results are called Asymptotic Modal Analysis (AMA). In reference [1], moreover, specific generalizations were made for structural-acoustic systems and interacting subsystems. Since AMA results can be derived systematically from CMA, AMA allows an assessment of the assumptions and consequent simplifications which are made to obtain such results and a combination of CMA and AMA (or SEA) may prove useful in applications.

In reference [3], the comparison of AMA (or SEA) and CMA was made for the response of a single general linear structure and the asymptotic characteristics of AMA were discussed. It was shown that the asymptotic behavior of AMA (or SEA) results depends upon the number of modes in a frequency interval of interest and the location of the point forces, and that, asymptotically, all points on the structure except for some special areas have the same response; the exceptional areas are near the points of excitation and near the structural system boundary. Some numerical examples for a beam were presented in reference [3].

In this paper an experimental study of the response of a rectangular plate under a point random force is reported. There were two objectives in this study. The first one was to demonstrate experimentally the manner in which the asymptotic limit is approached. The second one was to show experimentally that the response of almost all points of the plate becomes the same in the asymptotic limit.

Similar experimental and theoretical investigations were carried out by Crandall *et al.* [4–6]. Their works were directed primarily toward the identification and verification of

† On leave from Toshiba Research and Development Center, Japan.

“intensification zones” or local peak responses. Since the input force level was not calibrated in the experiments, no quantitative comparison between calculated and measured response levels of the SEA type could be made. Moreover asymptotic behavior of the response as the frequency bandwidth increases was not studied experimentally.

Experimental measurements, as described in this paper, have been carried out for several frequency bandwidths in which the maximum one corresponds to 47.1 modes of plate vibration, for several band center frequencies, and for two locations of the point force which are the center of the plate and near the plate edge, respectively.

All experimental results verify the asymptotic behavior of the plate response which is predicted by AMA.

2. BRIEF REVIEW OF AMA AND A NUMERICAL EXAMPLE

By using classical modal analysis the mean square response of a plate under many point random forces can be calculated by the following equation, on the assumption that the damping is small and the external forces are nearly white noise, see reference [7]:

$$\bar{w}^2(x, y) \cong \frac{\pi}{4} \sum_m \frac{\psi_m^2(x, y)}{M_m^2 \omega_m^3 \zeta_m} \sum_i \sum_j \psi_m(x_i, y_i) \psi_m(x_j^*, y_j^*) \Phi_{F_{ij}}(\omega_m). \quad (1)$$

All terms are defined in Appendix C. When a spatial average over the response is taken, equation (1) becomes

$$\langle \bar{w}^2 \rangle \cong \frac{\pi}{4} \sum_m \frac{\langle \psi_m^2 \rangle}{M_m^2 \omega_m^3 \zeta_m} \sum_i \sum_j \psi_m(x_i, y_i) \psi_m(x_j^*, y_j^*) \Phi_{F_{ij}}(\omega_m), \quad (2)$$

where $\langle \rangle$ denotes a spatial average. Note that the point pairs x_i, y_i, x_j^*, y_j^* obey $x_i = x_i^*, y_i = y_i^*$: i.e., they range over the same points on the plate. Hence the * superscript is superfluous.

If the number of modes is large then the right-hand side of equation (2) will tend to be dominated by terms for which $i = j$. Hence equation (2) becomes

$$\langle \bar{w}^2 \rangle \cong \frac{\pi}{4} \sum_m \frac{\langle \psi_m^2 \rangle}{M_m^2 \omega_m^3 \zeta_m} \sum_{i=1}^I \psi_m^2(x_i, y_i) \Phi_{F_{ii}}(\omega_m), \quad (3)$$

where I is the number of the point forces.

In a certain interval of frequency, $M_m^2, \omega_m^3, \zeta_m, \Phi_{F_{ii}}(\omega_m)$, and $\langle \psi_m^2 \rangle$ will be slowly varying with mode number, m , but $\psi_m^2(x_i, y_i)$ will vary relatively rapidly. Thus, in a certain interval of frequency, $\Delta\omega$,

$$\langle \bar{w}^2 \rangle \cong \frac{\pi}{4} \frac{\langle \psi_c^2 \rangle}{M_c^2 \omega_c^3 \zeta_c} \sum_{i=1}^I \Phi_{F_{ii}}(\omega_c) \sum_m \psi_m^2(x_i, y_i), \quad (4)$$

where the subscript c denotes the center frequency in the interval, $\Delta\omega$. But now, if there is a large number of modes, ΔM , in the frequency interval, $\Delta\omega$, then

$$\sum_{m=M}^{M+\Delta M-1} \psi_m^2(x_i, y_i) \cong \Delta M \langle \psi_c^2 \rangle. \quad (5)$$

Thus,

$$\langle \bar{w}^2 \rangle_{\Delta\omega} = \frac{\pi}{4} \frac{\Delta M}{\Delta\omega} \frac{\langle \psi_c^2 \rangle^2}{M_c^2 \omega_c^3 \zeta_c} \left[\sum_{i=1}^I \Phi_{F_{ii}}(\omega_c) \Delta\omega \right], \quad (6)$$

where $[\sum_{i=1}^I \Phi_{F_{ii}}(\omega_c) \Delta\omega] \cong \langle \bar{F}^2 \rangle_{\Delta\omega}$ may be identified as the total (mean square) force of the point forces in the frequency interval, $\Delta\omega$. Moreover, if the plate mass per area is

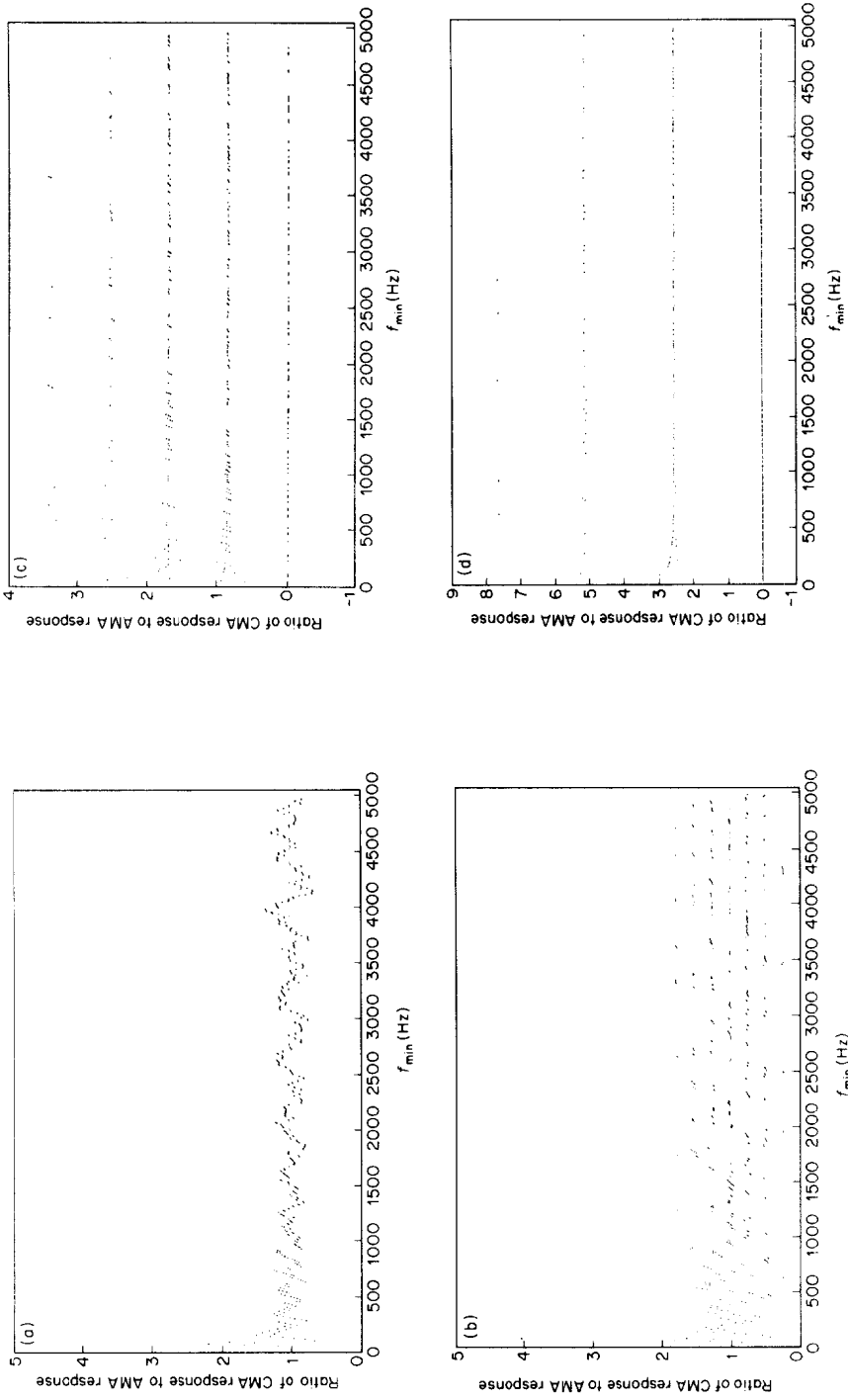


Figure 1. Ratio of CMA response to AMA response versus minimum frequency for $x_1 = y_1 = 0.5$. (a) $\Delta f = 300$ Hz; (b) $\Delta f = 100$ Hz; (c) $\Delta f = 30$ Hz; (d) $\Delta f = 10$ Hz.

smoothly varying, then the plate generalized mass at the center frequency may be written as $M_c \equiv M_p \langle \psi_c^2 \rangle$, where M_p is the total plate mass.

Hence, finally, if there are many modes (large ΔM) in $\Delta\omega$, then equation (6) may be written as

$$\langle \bar{w}^2 \rangle_{\Delta\omega} = (\pi/4)(\Delta M / \Delta\omega) (\langle \bar{F}^2 \rangle_{\Delta\omega} / M_p^2 \omega_c^3 \zeta_c). \tag{7}$$

Equation (7) is the final result of AMA for the response of a plate under point random forces. For a more detailed derivation and discussion, see reference [3]. Note here that equation (7) is not only the asymptotic limit for the spatial average of the plate response, but also the correct asymptotic limit for the response at almost *any* spatial point on the plate. For the discussion about the exceptional points, see Appendix A.

Taking the ratio of equation (2) to equation (7) one has a measure of goodness of the asymptotic approximation, $\langle \bar{w}^2 \rangle_{\text{CMA}} / \langle \bar{w}^2 \rangle_{\text{AMA}}$. Now, for a numerical example, consider a uniform, all simply supported rectangular plate where $\psi_m = \sin m_x \pi x \sin m_y \pi y$; x, y are non-dimensionalized by plate length and width. A few sample calculations have been made for an aluminum plate under one point force, $I = 1$, whose dimensions are $762 \times 508 \times 0.794$ (in mm). These dimensions are the same as those of the plate which was used in the experiment (see the following section). In the calculation, the center frequency of the interval was defined as $f_c = (f_{\min} f_{\max})^{1/2}$ and the number of modes in the frequency interval, Δf , was estimated from $\Delta M \equiv \Delta f A_p / h \sqrt{3\rho/E}$, where A_p is the plate area and h the plate thickness. This equation is derived in reference [2].

In Figure 1 the ratio of CMA response to AMA response is given as a function of f_{\min} for $x_1 = y_1 = 0.5$. Figure 1(a) shows the ratio for $\Delta f = 300$ Hz, (b) for $\Delta f = 100$ Hz, (c) for $\Delta f = 30$ Hz, and (d) for $\Delta f = 10$ Hz. The number of modes, ΔM , in the frequency interval is approximately 47.1 for $\Delta f = 300$ Hz, 15.7 for $\Delta f = 100$ Hz, 4.7 for $\Delta f = 30$ Hz, and 1.6 for $\Delta f = 10$ Hz. The ratio oscillates about unity more randomly in the case of a plate than in the case of a beam (see reference [3]). The reason is that the mode numbers, m_x and m_y , do not form a single monotonic frequency sequence for a plate. However, the ratio approaches one as the frequency interval, Δf , becomes large. In the case of $\Delta f = 30$ Hz and $\Delta f = 10$ Hz, the ratio is sometimes zero when all m_x and/or m_y in the frequency interval, Δf , are even, i.e., all modes of the plate vibration in one or both directions are antisymmetric, and $x_1 = y_1 = 0.5$.

In Figure 2 the ratio of CMA results to AMA results is shown for $\Delta f = 300$ Hz and $x_1 = y_1 = 0.05$. This result is representative in that the asymptote is approached less rapidly when the location of the point force is near the plate edge: compare Figures 1(a) and 2.

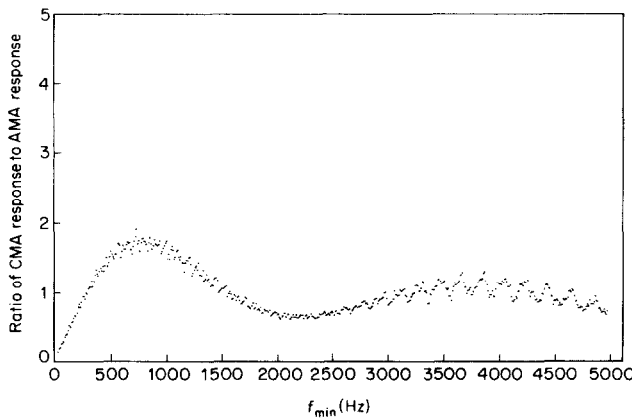


Figure 2. Ratio of CMA response to AMA response versus minimum frequency for $x_1 = y_1 = 0.05$ and $\Delta f = 300$ Hz.

3. EXPERIMENT

3.1. EXPERIMENTAL ARRANGEMENT

A schematic diagram of the experimental set-up is illustrated in Figure 3. The dimensions of the aluminum plate are $762 \times 508 \times 0.794$ (in mm). Small permeable discs (9 mm in diameter) are glued at the locations of excitation. Two opposite sides of the plate are clamped and the others are free, as shown in Figure 4. The first natural frequency of the

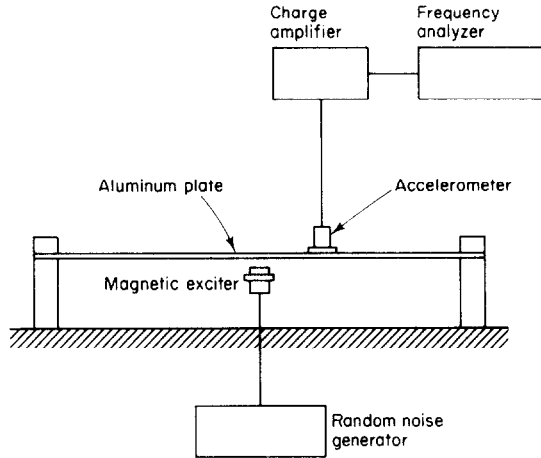


Figure 3. Experimental set-up.

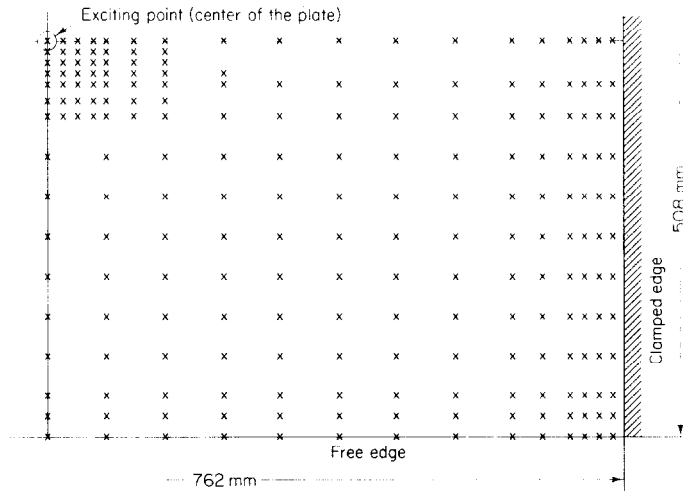


Figure 4. Plate dimension and measuring points for $x_1 = y_1 = 0.5$; \times , measuring points.

plate is determined to be 6.56 Hz experimentally and 6.74 Hz analytically, which was calculated from Janich's equation [8]. Figure 5 shows the damping ratio of the plate which was obtained by measurement. In the damping measurement the decrements of free vibration at each natural frequency were measured by using a frequency filter. Measurements were made at those points of the plate which had the maximum response, and averages were then taken. A non-contact magnetic transducer, Bruel & Kjaer (B&K) MM 0002, was used as a vibration exciter. The force level of the exciter was calibrated

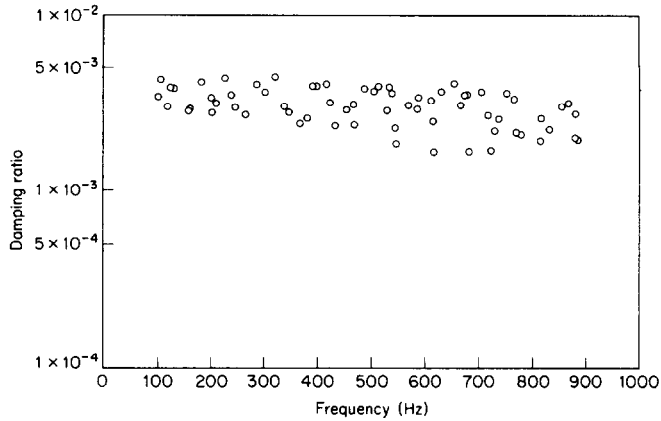


Figure 5. Damping ratio of the plate.

by a standard experimental set-up. The exciter force level depends upon the input voltage and the clearance between the exciter and the plate. However, those relationships are linear over the force level range which was used in the experiment. An example of the frequency response of the exciter force level is shown in Figure 6. The force level does not change very much with respect to frequency.

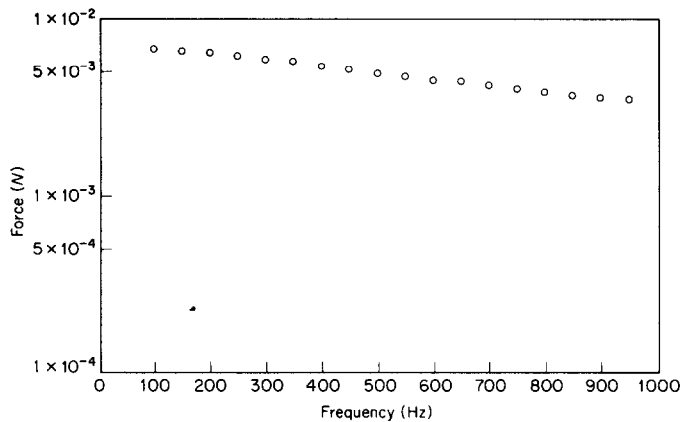


Figure 6. Force level of the magnetic exciter; 0.7 mm is the clearance between the exciter and the object, and 35 volt is the input voltage.

The exciter was driven by a random generator, B&K 1024. The frequency bandwidth of the narrow band random noise can be chosen in four steps, 10, 30, 100 and 300 Hz. The center frequency of the band noise can be tuned continuously. A small accelerometer, B&K 4375, whose weight is 3 g was used to detect the response of the plate. For measurement of higher order plate modes, the mass of the contact transducer has to be small, because for higher modes the measured value may be affected substantially by the transducer mass. This phenomenon can be predicted analytically for simple physical configurations: see Appendix B. Hence, one cannot measure accurately the response of the structure by a contact transducer for sufficiently high order modes, even if the transducer mass is small. The root mean square value of the plate response acceleration was measured by an accelerometer, B&K 4375, charge amplifier, B&K 2635, and frequency analyzer, B&K 2107.

3.2. EXPERIMENTAL MEASUREMENTS

Measurements have been performed for two locations of the exciting force, i.e., $x_1 = y_1 = 0.5$ and $x_1 = y_1 = 0.05$, where x_1 and y_1 are normalized by the length and width of the plate. For $x_1 = y_1 = 0.5$ (the exciting point is at the center of the plate) measurements have been made for four frequency bandwidths, $\Delta f = 10, 30, 100$ and 300 Hz, and for seven center frequencies, $f_c^* = 350, 400, 450, 500, 550, 600$ and 650 Hz, where f_c^* is defined as $f_c^* \equiv (f_{\min} + f_{\max})/2$. Measuring points on the plate are shown in Figure 4. Measurements have been made only for one quarter of the plate for $x_1 = y_1 = 0.5$.

For $x_1 = y_1 = 0.05$, measurements have been performed for $\Delta f = 300$ Hz and for four center frequencies, $f_c^* = 350, 450, 550$ and 650 Hz. Measuring points were similar to those shown in Figure 2: i.e., detailed measurements have been made for near the exciting point and near the plate edge, but now also for the whole plate.

The root mean square values of the plate response acceleration were measured directly. However, the mean square values of the local response acceleration and the spatial averages of the mean square acceleration value will be used in the following discussion. The spatial average has been calculated by averaging the average mean square value of each area which is surrounded by four measuring points.

3.3. EXPERIMENTAL RESULTS AND DISCUSSION

The ratio of experimental results to AMA results will be used to focus the following discussion. AMA results were calculated from equation (7) and the spatial average of the plate acceleration was defined by $\langle \bar{w}^2 \rangle_{\Delta\omega} = \omega_c^4 \langle \bar{w}^2 \rangle_{\Delta\omega}$ where $\omega_c \equiv (\omega_{\min} \omega_{\max})^{1/2}$. To determine the effective damping ratio, ζ_c , at the center frequency, the averages of the experimental damping data (see Figure 5) in each bandwidth 300 Hz were used for each $\Delta f = 300$ Hz, and the averages in each bandwidth 100 Hz were used for each $\Delta f = 10, 30$ and 100 Hz. These were used in the theoretical calculations.

The ratio of experimental results to AMA results versus the center frequencies is shown for various Δf in Figure 7. The ratio oscillates about one as the center frequency varies, but for larger Δf the variation is less. In Figure 8 the ratio of experimental results to AMA results versus the frequency bandwidth, Δf , is shown for $x_1 = y_1 = 0.5$. The bounded bar lines indicate the maximum and the minimum values determined by numerical calculations for various center frequencies in the corresponding frequency range for an all simply supported plate (see the previous section). Note here that the boundary

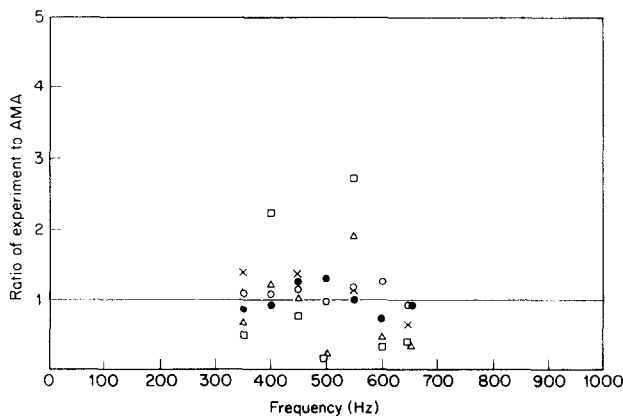


Figure 7. Ratio of experimental results to AMA results versus center frequency. $x_1 = y_1 = 0.5$; \circ , $\Delta f = 300$ Hz; \bullet , $\Delta f = 100$ Hz; \triangle , $\Delta f = 30$ Hz; \square , $\Delta f = 10$ Hz. $x_1 = y_1 = 0.05$; \times , $\Delta f = 300$ Hz.

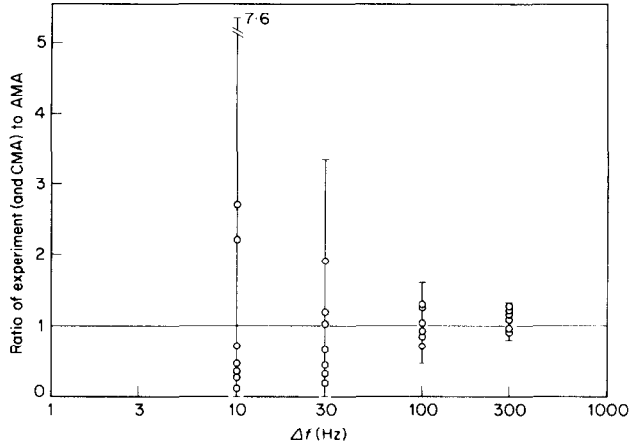


Figure 8. Ratio of experimental results (and CMA) to AMA results versus frequency interval for $x_1 = y_1 = 0.5$; various center frequencies. I, Theory, CMA/AMA; O, experiment/AMA.

condition of the plate used in the numerical examples is different from that in the experiment. For a high mode, however, the natural mode shapes will tend to be independent of boundary support conditions: see references [9] and [10]. Hence, for the higher modes, the asymptotic behavior of equation (5) will not change even if the boundary condition of the plate is changed. As can be seen from Figure 8, both experimental and numerical results approach one as the frequency bandwidth, Δf , becomes large. It is interesting to note that all experimental results are bounded by the bar lines which describe the numerical result. Note that the experimental measurements have been made for seven center frequencies.

In Figure 9 the ratio of experimental (and numerical CMA) results to AMA results versus the location of the exciting point, $x_1 = y_1$, is shown for $\Delta f = 300$ Hz. AMA is less accurate when the location of the point force is near the plate edge.

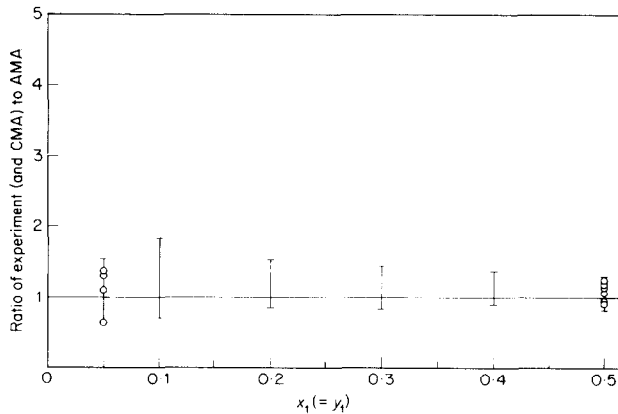


Figure 9. Ratio of experimental results (and CMA) to AMA results versus location of force for $\Delta f = 300$ Hz. Key as Figure 8.

The distributions of the plate response for various Δf and $f_c^* = 650$ Hz are shown in Figure 10. Figure 10(a) shows the case of $\Delta f = 10$ Hz, (b) for $\Delta f = 30$ Hz, (c) for $\Delta f = 100$ Hz, and (d) for $\Delta f = 300$ Hz. The vertical axis in Figure 10 shows the ratio of the mean square local response to the spatial average of the mean square response,

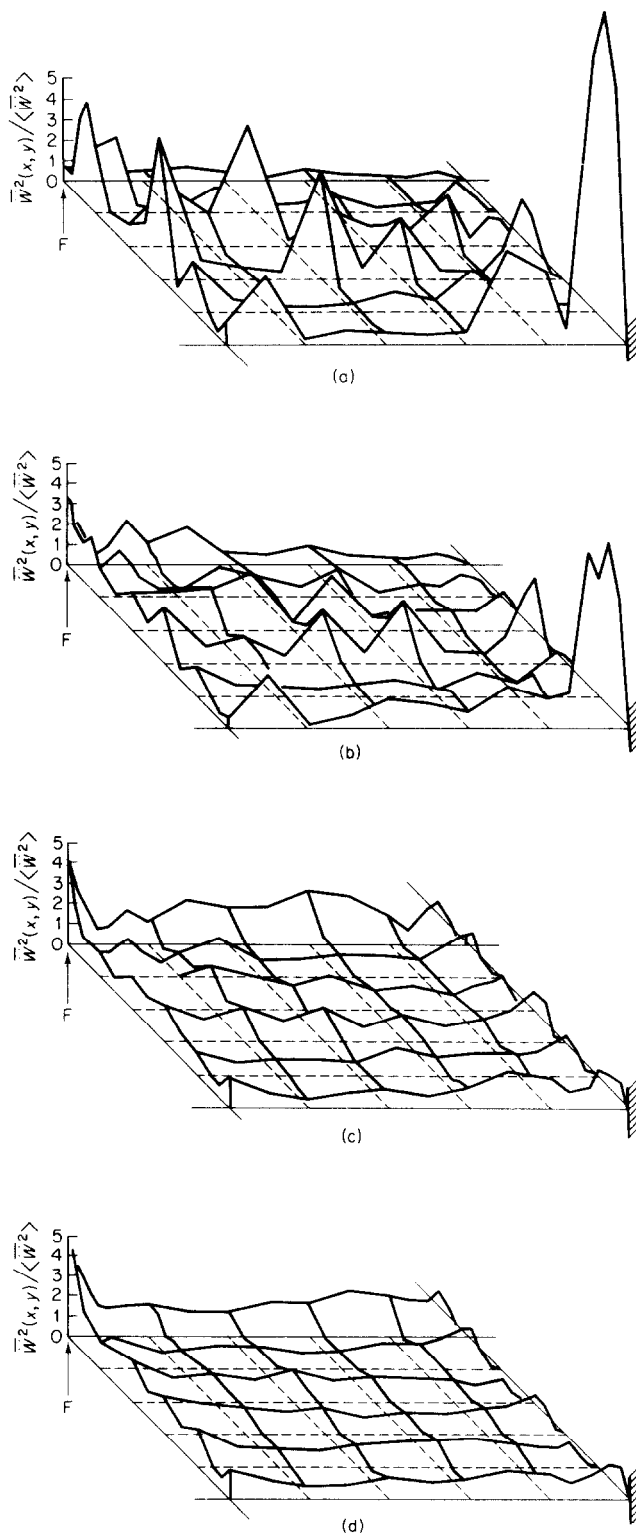


Figure 10. Ratio of mean square local response to spatial average of mean square response for $x_1 = y_1 = 0.5$ and $f_c^* = 650$ Hz; (a) $\Delta f = 10$ Hz; (b) $\Delta f = 30$ Hz; (c) $\Delta f = 100$ Hz; (d) $\Delta f = 300$ Hz.

$\bar{w}_{\Delta\omega}^2(x, y)/\langle\bar{w}^2\rangle_{\Delta\omega}$. In the case of $\Delta f = 300$ Hz, the accelerations of all points of the plate except for some selected areas are almost the same as the spatial average. The exceptional areas are near the lines $x = x_1$ and $y = y_1$, and near the edge of the plate. According to AMA (see Appendix A), the points on $x = x_1$ or $y = y_1$ have a response twice as large as the spatial average in the asymptotic limit and the response at the location of the point force becomes asymptotically four times as large as the spatial average. For more discussion about the asymptotic limit of the exceptional areas, see Appendix A. Experimental results for $\Delta f = 300$ Hz show good agreement with these analytical asymptotic limits. These analytical results are some of the generalizations of AMA beyond SEA. As can be seen from Figure 10(a)-(d) the spatial distribution of the plate response will vary less as the frequency bandwidth, Δf , becomes large.

4. CONCLUDING REMARKS

Experimental investigations of the accuracy of AMA have been performed for the response of a rectangular plate under a point random force and the following conclusions have been reached.

(1) The response of the plate approaches its asymptotic limit as the frequency interval becomes large, but when the exciting point is near the plate edge the response varies more from its asymptotic limit. Typically the frequency interval must contain 20–50 modes for the asymptotic limit to be a useful approximation.

(2) All points of the plate except for some selected areas have nearly the same response when the frequency interval is large. The exceptional areas are near the lines of $x = x_i$ and $y = y_i$, and near the plate edge. x_i, y_i is the position of the point random force. For $x_i = y_i = 0.5$ the response of points on $x = x_i$ or $y = y_i$ is almost twice as large as the average response and the response at the exciting point is almost four times as large as the spatial average when the frequency interval is large.

These experimental results are predicted by AMA. It has been verified experimentally that AMA is a valid, consistent, and useful approximation as Δf becomes sufficiently large.

REFERENCES

1. E. H. DOWELL 1983 *United Technologies Research Center R82-112247*. Vibration induced noise on aircraft: asymptotic modal analysis and statistical energy analysis of dynamical systems.
2. R. H. LYON 1975 *Statistical Energy Analysis of Dynamical Systems: Theory and Application*. Cambridge, Massachusetts: MIT Press.
3. E. H. DOWELL and Y. KUBOTA 1984 *American Society of Mechanical Engineers Journal of Applied Mechanics*. Asymptotic modal analysis and statistical energy analysis of dynamical systems.
4. S. H. CRANDALL 1979 in *Developments in Statistics* Volume 2 (editor P. R. Krishnaiah). New York: Academic Press, 1–82. Random vibration of one- and two-dimensional structures.
5. K. ITAO and S. H. CRANDALL 1978 *American Society of Mechanical Engineers Journal of Mechanical Design* **100**, 690–695. Wide-band random vibration of circular plates.
6. S. H. CRANDALL and A. P. KULVETS 1977 in *Application of Statistics* (editor P. R. Krishnaiah). North-Holland, 163–182. Source Correlation Effects on Structural Response.
7. Y. K. LIN 1967 *Probabilistic Theory of Structural Dynamics*. New York: McGraw-Hill.
8. A. W. LEISSA 1969 *NASA SP-160*. Vibration of plates.
9. V. V. BOLOTIN 1961 *Problems of Continuum Mechanics SIAM* 56–68. An asymptotic method for problem of eigenvalues for rectangular regions.
10. E. H. DOWELL 1984 *American Society of Mechanical Engineers Journal of Applied Mechanics* **51**, 439. On asymptotic approximations to beam modal shapes.

APPENDIX A: ASYMPTOTIC LIMIT OF LOCAL RESPONSE

Equation (7) was derived by starting from equation (1). As a first step a spatial average of equation (1) was taken leading to equation (2). What is perhaps remarkable is that it can be shown that equation (7) is also the correct asymptotic limit for the response at *almost* any spatial point on the plate. Some special points, however, have other asymptotic limits. A brief discussion of the asymptotic limit of the local response follows.

Consider equation (1) and retain only those terms for which $i = j$ since asymptotically these will be dominant. In a certain frequency interval M_m^2 , ω_m^2 , ζ_m , $\phi_{F_i}(\omega_m)$ will be slowly varying with the mode number, m , but $\psi_m^2(x, y)$ and $\psi_m^2(x_i, y_i)$ will vary relatively rapidly. Then equation (1) becomes

$$\bar{w}^2(x, y) \cong \frac{\pi}{4} \frac{1}{M_c^2 \omega_c^3 \zeta_c} \sum_i \Phi_{F_i}(\omega_c) \sum_m \psi_m^2(x, y) \psi_m^2(x_i, y_i). \quad (\text{A1})$$

Compare equation (A1) and equation (4). Equation (4) is for the spatial average response, while equation (A1) is for the response at any point, x, y . It can be shown that

$$\sum_{m=M}^{M+\Delta M-1} \psi_m^2(x, y) \psi_m^2(x_i, y_i) \rightarrow [\langle \psi_m^2 \rangle]^2 \Delta M \quad (\text{A2})$$

for $\Delta M \rightarrow \infty$ for most x, y and x_i, y_i .

Recall here that the plate mode functions can be represented as the product of beam functions (see reference [8]); that is, $\psi_m(x, y) = x_r(x)y_s(y)$, where $x_r(x)$ and $y_s(y)$ are chosen as the mode shapes of beams having the boundary conditions of the plate. This is exact for a pinned-pinned plate and asymptotically correct for other boundary conditions. Moreover, if the number of modes is sufficiently large, then

$$[(1/\Delta r) \sum_r x_r^2(x)x_r^2(x_i)] [(1/\Delta s) \sum_s y_s^2(y)y_s^2(y_i)] \rightarrow [\langle x_r^2 \rangle]^2 [\langle y_s^2 \rangle]^2 = [\langle \psi_m^2 \rangle]^2 \quad (\text{A3})$$

as $\Delta r, \Delta s \rightarrow \infty$, where Δr and Δs are the number of modes in the x and y directions. Hence, it is sufficient to consider the asymptotic limits for the beam functions.

As an example, consider the natural modes of a uniform, simply supported beam of length L ($x_r(x) = \sin(r\pi x)/L$). The results of $S_r \equiv [\sum_{r=r_0}^{r_0+\Delta r-1} x_r^2(x)x_r^2(x_i)]$ are obtained analytically and the asymptotic limits are given in the following.

(I) When $x \neq 0, L/2, L, x_i$,

$$(\Delta r/4) - R_I \leq S_r \leq (\Delta r/4) + R_I, \quad (\text{A4})$$

where

$$R_I \equiv \left| \sin \frac{\Delta r \pi (x + x_i)}{L} / 8 \sin \frac{\pi (x + x_i)}{L} \right| + \left| \sin \frac{\Delta r \pi (x - x_i)}{L} / 8 \sin \frac{\pi (x - x_i)}{L} \right| \\ + \left| \sin \frac{\Delta r \pi x}{L} / 4 \sin \frac{\pi x}{L} \right| + \left| \sin \frac{\Delta r \pi x_i}{L} / 4 \sin \frac{\pi x_i}{L} \right|.$$

Hence

$$\lim_{\Delta r \rightarrow \infty} (1/\Delta r) S_r = \frac{1}{4} (= [\langle x_r^2 \rangle]^2) \quad (\text{A5})$$

(II) When $x = x_i \neq L/2$,

$$\frac{3}{8} \Delta r - R_{II} \leq S_r \leq \frac{3}{8} \Delta r + R_{II}, \quad (\text{A6})$$

where $R_{II} \equiv |\sin(\Delta r \pi x_i/L)/2 \sin(\pi x_i/L)| + |\sin(2\Delta r \pi x_i/L)/8 \sin(2\pi x_i/L)|$.

Hence

$$\lim_{\Delta r \rightarrow \infty} (1/\Delta r)S_r = \frac{3}{8} (= \frac{3}{8}[\langle x_r^2 \rangle]^2). \quad (\text{A7})$$

(III) When $x = x_i = L/2$,

$$S_r = \Delta r/2 + [1 - (-1)^{\Delta r}]/4. \quad (\text{A8})$$

Hence

$$\lim_{\Delta r \rightarrow \infty} (1/\Delta r)S_r = \frac{1}{2} (= 2[\langle x_r^2 \rangle]^2). \quad (\text{A9})$$

Thus, in cases (II) and (III), equation (A2) does not follow. For $x = x_i$ and/or $y = y_i$, the right-hand side of equation (A2) should be multiplied by $(3/2)^D$ for $x_i \neq L/2$ and/or $y_i \neq L/2$, and by 2^D for $x = L/2$ and/or $y = L/2$ where $D = 1$ or 2 for one or two dimensions, respectively. Recall that, for a high mode, the mode shapes will tend to be independent of boundary conditions except near the boundary: see references [9] and [10]. Therefore, these asymptotic results are also correct for the other boundary conditions except for the case that x , x_i , y , and y_i are near the boundary: see Figure 10.

Of course, equation (A2) does not follow for response points near the boundary. As a special case, consider the case when x/L is very small, i.e., near the edge, and $\Delta r\pi x/L$ is also very small. In this case the result of the summation, S_r , is bounded by

$$\frac{\Delta r}{4} \left[1 - \cos \frac{(2r_0 + \Delta r - 1)\pi x}{L} \right] - R_B \leq S_r \leq \frac{\Delta r}{4} \left[1 - \cos \frac{(2r_0 + \Delta r - 1)\pi x}{L} \right] + R_B, \quad (\text{A10})$$

$$\text{where } R_B \equiv \left| \sin \frac{\Delta r\pi(x+x_i)}{L} \right| / \left| 8 \sin \frac{\pi(x+x_i)}{L} \right| + \left| \sin \frac{\Delta r\pi(x-x_i)}{L} \right| / \left| 8 \sin \frac{\pi(x-x_i)}{L} \right| \\ + \left| \sin \frac{\Delta r\pi x_i}{L} \right| / \left| 4 \sin \frac{\pi x_i}{L} \right|.$$

Hence, when $r_0/\Delta r$ is sufficiently large and $(2r_0 + \Delta r - 1)x/L = 1$,

$$\lim_{\Delta r \rightarrow \infty} (1/\Delta r)S_r = \frac{1}{2} (= 2[\langle x_r^2 \rangle]^2). \quad (\text{A11})$$

Therefore, the response at $x = L/(2r_0 + \Delta r - 1)$ becomes twice as large as the spatial average response in the asymptotic limit. It is interesting to note that $L/(2r_0 + \Delta r - 1)$ is one quarter of the average wave length in the frequency interval. Though the boundary for the plate which was used in the experiment is not simply supported, a similar phenomenon for response near the clamped edge is observed in Figure 10.

APPENDIX B: EFFECT OF TRANSDUCER MASS

To study the effect of a transducer mass, consider a high mode of a uniform, simply supported beam of length L . For the sake of simplicity, it is assumed that the transducer is placed at a point, x_0 , at which the slope of the deflection is zero.

The differential equation of motion is

$$EI\partial^4 w/\partial x^4 = -m_B\partial^2 w/\partial t^2, \quad (\text{B1})$$

where w is the beam deflection, EI is the flexural rigidity, and m_B is the mass per unit length of the beam. Now assume a solution of equation (B1) in the form

$$w(x, t) = w(x) e^{i\omega t}. \quad (\text{B2})$$

Thus

$$w'''' = \beta w, \quad (\text{B3})$$

where $\beta \equiv m_B \omega^2 / EI$. The boundary conditions for the region $0 \leq x \leq x_0$ are

$$w(0) = w''(0) = 0, \quad w'(x_0) = 0, \quad EI w'''(x_0) = -(m_A \omega^2 / 2) w(x_0), \quad (\text{B4})$$

where m_A is the transducer mass. Using boundary conditions (B4), one obtains the characteristic equation

$$\cos \beta x_0 \cosh \beta x_0 + (\beta L / 4)(m_A / M_B) [\cos \beta x_0 \sinh \beta x_0 - \sin \beta x_0 \cosh \beta x_0] = 0 \quad (\text{B5})$$

and the mode shape function

$$w(x) = \sin \beta x + \frac{[\cos \beta x_0 - (\beta L / 2)(m_A / M_B) \sin \beta x_0]}{[\cosh \beta x_0 + (\beta L / 2)(m_A / M_B) \sinh \beta x_0]} \sinh \beta x, \quad (\text{B6})$$

where M_B is the total mass of the beam. Since βx_0 is very large for a high mode,

$$\cosh \beta x_0 \cong \sinh \beta x_0 (\cong \frac{1}{2} e^{\beta x_0}). \quad (\text{B7})$$

Hence, the characteristic equation (B5) becomes approximately

$$\cos(\beta x_0 - \theta) = 0, \quad (\text{B8})$$

where $\theta \equiv \tan^{-1} \{-(\beta L / 4)(m_A / M_B) / [1 + (\beta L / 4)(m_A / M_B)]\}$. Equation (B8) yields the eigenvalues

$$\beta_r x_0 = (r\pi - \pi/2) - \phi_r \quad r = 1, 2, \dots, \quad (\text{B9})$$

where $\phi_r \equiv \tan^{-1} \{-(\beta_r L / 4)(m_A / M_B) / [1 + (\beta_r L / 4)(m_A / M_B)]\}$, $0 < \phi_r < \pi/4$. By using equations (B6), (B7) and (B9), the normalized amplitude of the response at x_0 can be obtained from

$$|w_r(x_0)| = \cos(\phi_r - \pi/4) / [1 + (r\pi/2)(L/x_0)(m_A / M_B)]. \quad (\text{B10})$$

The amplitude at x_0 becomes smaller as r and/or m_A becomes large. Equation (B10) indicates that the value detected by the transducer is always smaller than the correct value which is the response without the transducer. Therefore, the transducer mass should be as small as possible in measurements. Equation (B10) may be used as a guide for how small the mass must be. However, note that one cannot measure accurately the correct value for *sufficiently* high modes by a contact transducer, even if the transducer mass is small but non-zero.

APPENDIX C: NOMENCLATURE

A_p	plate area
E	modulus of elasticity
F	force
Δf	frequency interval in Hz
f_{\max}	maximum frequency in Δf
f_{\min}	minimum frequency in Δf
f_c	center frequency of Δf , $\equiv (f_{\min} f_{\max})^{1/2}$
f_c^*	center frequency of Δf , $\equiv (f_{\min} + f_{\max})/2$
h	plate thickness
I	number of forces
M	first mode number in the frequency interval, $\Delta\omega$
M_m	plate generalized mass, $\equiv \iint m_p \psi_m^2 dx dy$
ΔM	number of plate modes in $\Delta\omega$

M_p	total mass of plate
m_p	plate mass per area
w	plate deflection
x, y	Cartesian co-ordinates
Φ	power spectral density
ψ_m	plate modal shape function
ρ	plate density
ζ_m	modal damping of plate
ω	frequency in radians per seconds
ω_m	modal frequency of plate
$\bar{\cdot}$	mean (temporal)
$\langle \cdot \cdot \cdot \rangle$	spatial average
i, j	subscripts denoting i th and j th points
$\Delta\omega$	subscript denotes property associated with the frequency interval $\Delta\omega$
c	subscript denotes property evaluated at center frequency of $\Delta\omega$